Trans Interactions between Galactosylceramide and Cerebroside Sulfate across Apposed Bilayers

Joan M. Boggs,*† Abdellah Menikh,* and Godha Rangaraj*
*The Research Institute, The Hospital for Sick Children, Toronto M5G 1X8, Canada and †Department of Laboratory Medicine and Pathobiology, University of Toronto, Toronto, Ontario M5G 1L5, Canada

ABSTRACT The two glycosphingolipids galactosylceramide (GalC) and its sulfated form, cerebroside sulfate (CBS), are present at high concentrations in the multilayered myelin sheath and are involved in carbohydrate-carbohydrate interactions between the lipid headgroups. In order to study the structure of the complex of these two glycolipids by Fourier transform infrared (FTIR) spectroscopy, GalC dispersions were combined with CBS dispersions in the presence and absence of Ca^{2+}. The FTIR spectra indicated that a strong interaction occurred between these glycolipids even in the absence of Ca^{2+}. The interaction resulted in dehydration of the sulfate, changes in the intermolecular hydrogen bonding interactions of the sugar and other oxygens, decreased intermolecular hydrogen bonding of the amide C═O of GalC and dehydration of the amide region of one or both of the lipids in the mixture, and disordering of the hydrocarbon chains of both lipids. The spectra also show that Ca^{2+} interacts with the sulfate of CBS. Although they do not reveal which other groups of CBS and GalC interact with Ca^{2+} or which groups participate in the interaction between the two lipids, they do show that the sulfate is not directly involved in interaction with GalC, since it can still bind to Ca^{2+} in the mixture. The interaction between these two lipids could be either a lateral *cis* interaction in the same bilayer or a *trans* interaction between apposed bilayers. The type of interaction between the lipids, *cis* or *trans*, was investigated using fluorescent and spin-label probes and anti-glycolipid antibodies. The results confirmed a strong interaction between the GalC and the CBS microstructures. They suggested further that this interaction caused the CBS microstructures to be disrupted so that CBS formed a single bilayer around the GalC multilayered microstructures, thus sequestering GalC from the external aqueous phase. Thus the CBS and GalC interacted via a *trans* interaction across apposed bilayers, which resulted in dehydration of the headgroup and interface region of both lipid bilayers. The strong interaction between these lipids may be involved in stabilization of the myelin sheath.

INTRODUCTION

Increasing evidence suggests that glycolipids play a fundamental role in recognition processes in cell development and cell-cell adhesion (Hakomori, 1984; 1991). Ca^{2+}-mediated interactions between the carbohydrates of glycolipids and glycoproteins on apposed surfaces can bridge those surfaces (Hakomori, 1991; Eggens et al., 1989; Misevic and Burger, 1993). Such interactions between apposed cell surfaces have recently been termed a "sugar zipper" (Spillman, 1994). A divalent cation-mediated interaction has been shown to occur between the two major glycosphingolipids of myelin, GalC, and its sulfated form, CBS, which make up 15 and 4 mol % of the lipid in myelin, respectively (Norton, 1977). This interaction may play a role in adhesion of the extracellular surfaces of myelin or in other more dynamic functions of myelin. It results in binding of liposomes containing GalC to a CBS-coated surface (Hakomori, 1991) and in aggregation of phosphatidylcholine/cholesterol liposomes containing GalC with similar liposomes containing CBS (Stewart and Boggs, 1993). The aggregation is reversible on addition of EDTA. Formation of a heterotypic complex between these two GSLs and Ca^{2+} also occurs in methanol, as detected by electrospray ionization mass spectrometry (Koshy and Boggs, 1996; Koshy et al., 1999).

Although interactions between these two glycolipids might also occur when they are present in the same bilayer (*cis* interaction), the interaction between them in apposed bilayers is a *trans* interaction. In the present study, dispersions of GalC were mixed with dispersions of CBS in the presence and absence of Ca^{2+} in order to study the structure of the Ca^{2+}-GalC-CBS complex by FTIR spectroscopy. Phosphatidylcholine and cholesterol were omitted in order to simplify the FTIR spectra. Interestingly, the results indicated that in the absence of these auxiliary lipids, a strong interaction occurred between these glycolipids even in the absence of Ca^{2+}. The type of interaction between the lipids, *cis* or *trans*, was investigated using fluorescent and spin-label probes and anti-glycolipid antibodies.

Received for publication 15 July 1999 and in final form 2 November 1999.

Address reprint requests to Dr. Joan M. Boggs, Division of Structural Biology and Biochemistry, The Research Institute, The Hospital for Sick Children, 555 University Ave., Toronto, Ontario M5G 1L5, Canada. Tel.: 416-813-5919; Fax: 416-813-5022; E-mail: jmboggs@sickkids.on.ca.

Abdellah Menikh's present address is Section of Molecular Biophysics/Chemical Physics, NIH, Bldg. 5, Bethesda, MD 20892-0520.

Abbreviations used: GalC, galactosylceramide; CBS, cerebroside sulfate; C18:0h-CBS, α-hydroxylated stearic acid species of CBS; DPPC, dipalmitoylphosphatidylcholine; egg PC, egg phosphatidylcholine; EPR, electron paramagnetic resonance spectroscopy; 5-S-SL, 5-doxyl-stearate; FTIR, Fourier transform infrared spectroscopy; HFA, hydroxy fatty acid species; HTEMPO, 4-(*N*,*N*-dimethyl-*N*-*n*-hexadecylammonio)-2,2,6,6-tetramethylpiperidine-1-oxyl iodide; NBD-PE, *N*-(7-nitrobenz-2-oxa-1,3-diazol-4-yl)-1,2-dihexadecanoyl-*sn*-glycero-3-phosphoethanolamine, triethylammonium salt; nCBS, natural bovine brain CBS; nGalC, natural bovine brain GalC; NFA, non-hydroxy fatty acid species; Rho-PE, *N*-(Lissamine rhodamine B sulfonyl)-1,2-dihexadecanoyl-*sn*-glycero-3-phosphoethanolamine, triethylammonium salt; 16-S-SL, 16-doxyl-stearate; TX-100, Triton X-100.

0006-3495/00/02/874/12 $2.00

MATERIALS AND METHODS

Materials

nGalC and HFA-nGalC were obtained from Supelco, Inc. (Bellefonte, PA). The latter gave a single spot by TLC and was used without further purification. C18:0h-CBS was prepared from bovine brain psychosine sulfate and stearoyl chloride as described earlier (Koshy and Boggs, 1983). In the absence of added cations it is in the NH_4^+ salt form (Koshy and Boggs, 1996). nCBS containing a mixture of NFA and HFA forms was purified as described (Boggs et al., 1988). Egg PC was purchased from Avanti Polar Lipids (Alabaster, AL). D_2O (99.9%) was obtained from Merck, Sharp, and Dohme (Montreal, Canada). $CaCl_2 \cdot 2H_2O$ was from Fisher (Fairlawn, NJ) and purified as described (Menikh and Fragata, 1993). [^{14}C]-DPPC (specific activity 110 mCi/mmol) was purchased from NEN (Boston, MA). Fluorescent probes Rho-PE and NBD-PE were purchased from Molecular Probes (Eugene, OR). HTEMPO was purchased from Molecular Probes; 5-S-SL and 16-S-SL were purchased from Aldrich (Milwaukee, WI). Rabbit antisera to CBS were raised as described (Crook et al., 1987). Rabbit anti-GalC antiserum was purchased from Sigma (St. Louis, MO). Goat anti-rabbit IgG labeled with ^{125}I (specific activity 15.5 μCi/μg) was purchased from ICN Pharmaceuticals, Inc. (Irvine, CA).

Sample preparation for FTIR spectroscopy

Aliquots of chloroform/methanol (2:1) solutions of HFA-nGalC or C18:0h-CBS were dried under a stream of nitrogen and then kept under vacuum overnight. The dried lipid was dispersed by vortex mixing at 90°C in either D_2O or H_2O to give a final lipid concentration of ~1 mg/ml. An aliquot of a 1 M solution of $CaCl_2$ was added to the dispersions in order to obtain a final Ca^{2+} concentration of 5 mM Ca^{2+}. For the combined GalC and CBS dispersions, Ca^{2+} was added after combining the dispersions. Both dry and hydrated samples were studied by infrared spectroscopy. Dry films were prepared by placing ~40 μl of lipid dispersion on a CaF_2 window and allowing it to dehydrate in a desiccator under vacuum for ~24 h. Hydrated samples were studied by sedimenting the lipid suspension by centrifugation in an Eppendorf centrifuge for 5 min. The supernatant was removed and the wet pellet was mounted between two CaF_2 windows.

FTIR measurements

Infrared spectra were measured in a Bruker FTIR spectrometer, model IFS 48, equipped with a germanium-coated KBr beam splitter and DTGS detector. Generally, 100 interferograms were collected, coadded, apodized, and Fourier transformed at a resolution of 2 cm^{-1} after subtraction of the CaF_2 plate reference spectrum. The spectrometer was continuously purged with nitrogen to eliminate spectral interference from water vapor. In order to separate unresolvable infrared band contours, a second derivatization and curve-fitting analysis were applied, and the resulting spectra were smoothed at 11 data points using Spectra Calc (Galactic Industries Corp., Salem, NH), which makes use of the Savitzky-Golay convolution method (Savitzky and Golay, 1964). During the curve-fitting procedure the positions of band maxima were obtained from the corresponding minima in the second derivative spectra. Each band was simulated by a Gaussian-Lorentzian function to achieve the best fit.

Sedimentation assay

nCBS and nGalC dispersions labeled with trace amounts of [^{14}C]-DPPC were prepared by mixing the nCBS or nGalC with 100,000 cpm [^{14}C]-DPPC per sample in solvent, evaporation of the solvent, and dispersion of the lipid in water as described above at a concentration of 1 mg lipid/100 μl for samples with single lipids, 1 mg nCBS plus 1 mg nGalC per 100 μl for premixed samples, or 1 mg nCBS/50 μl and 1 mg nGalC/50 μl for dispersions to be combined. In the last case, the [^{14}C]-DPPC was incorporated into the nCBS for combining with unlabeled nGalC dispersions and into the nGalC for combining with unlabeled nCBS dispersions. After combining nCBS and nGalC dispersions, samples were incubated at 4°C for 1 h or overnight. Similar results were obtained for both incubation times. Most samples were then diluted to 1 ml, centrifuged at 4°C for 15 min in an Eppendorf bench centrifuge, and duplicate aliquots from the supernatant were added to ReadySafe scintillation fluid (Beckman) and counted for ^{14}C in a Beckman LS 60001C liquid scintillation counter. Some samples of combined dispersions in 100 μl final volume were evaporated under a stream of nitrogen and evacuated in a desiccator overnight to mimic the method of preparation of dry films for FTIR spectroscopy. They were then redispersed in 1 ml water by vigorous Vortex mixing at room temperature, centrifuged as above, and the supernatant counted for ^{14}C. More dilute samples containing 0.5–1 mg lipid were dispersed and incubated as above in a volume of 1 ml and centrifuged without further dilution.

Fluorescent probe assays for lipid mixing

Fluorescent probes were used to determine whether lipid mixing occurred as described (Hoekstra and Duzgunes, 1993). For samples where all of the nCBS added to the nGalC was labeled, nCBS containing 0.8 mol % each of Rho-PE and NBD-PE were prepared by dissolving the lipid and probes together in solvent, evaporating the solvent, and dispersing the lipid in water as described above at lipid concentrations of 0.5–10 mg/ml as indicated in the Tables. Unlabeled nGalC dispersions were similarly prepared. For combined nCBS and nGalC dispersions, aliquots of each dispersion were combined and incubated at 4°C for 1 h or overnight. Some samples were evaporated and redispersed in 1 ml of water as described above. Premixed nCBS-nGalC dispersions containing the same concentration of nCBS and nGalC as in the combined dispersions and 0.4 mol % of each probe with respect to the total lipid were prepared by dissolving both glycolipids and probes together in solvent, evaporating the solvent, and dispersing the lipid in water. After incubation, the more concentrated samples (10 mg/ml) were diluted to 1 ml by addition of water. The less concentrated (0.5–1 mg/ml) were already in 1 ml water. When unlabeled nCBS dispersions were also combined with the labeled nCBS dispersions and unlabeled nGalC dispersions, a separate dispersion of unlabeled nCBS was prepared, and labeled nCBS, unlabeled nCBS, and unlabeled nGalC dispersions were combined in a mole ratio of 1:4:5. Some of these samples were pelleted by centrifugation in an Eppendorf bench centrifuge and resuspended in the same supernatant or in the same volume of fresh water.

For measurement of fluorescence an aliquot of each sample was diluted 50% with water or with 2% TX-100. The fluorescence emission of NBD-PE at 530 nm was measured on a Perkin-Elmer LS30 fluorescence spectrometer with excitation at 460 nm. The peak excitation and emission wavelengths of Rho-PE are at ~570 and 585 nm, respectively. However, overlap between the emission spectrum of NBD and the excitation spectrum of Rho allows energy transfer from NBD to Rho to occur resulting in decreased emission of NBD at 530 nm. Fluorescence in TX-100 was corrected for quenching and considered to correspond to 100% probe dilution. The percent dilution for the dispersions in water was determined by dividing the emission of the sample in water by the emission in TX-100, multiplied by 100. The value obtained for labeled nCBS dispersions alone was considered to correspond to 0% dilution and was subtracted from all other values.

Accessibility of HTEMPO to ascorbate

nCBS, nGalC, and premixed nCBS-nGalC dispersions containing 1 mol % HTEMPO, at a concentration of 1 mg lipid/100 μl water, were prepared as described above. nCBS dispersions were combined with nGalC dispersions and incubated at a concentration of 1 mg of each lipid per 200 μl at 4°C

for 1 h. For the dispersions to be combined, the HTEMPO was included in either the nCBS dispersions or the nGalC dispersions at a concentration of 2 mol % HTEMPO so that if mixing of the two lipids occurred, the final concentration would be 1 mol %. Each sample was divided in half, put on ice, and 10 μl of 5 mM freshly made, cold sodium ascorbate was added to one half. The samples were taken up in 50 μl microcapillary tubes and kept on ice for immediate measurement of the EPR spectrum. The EPR spectrum was measured at 7°C on a Varian E104B EPR spectrometer equipped with a Varian temperature controller. Most of the HTEMPO inserts into the bilayer, giving a broad EPR spectrum typical of a motionally restricted spin label, while some is free in solution, giving a sharp three-line spectrum typical of isotropic motion. The EPR signal due to membrane-bound probe was measured from the height of the low-field broad peak, and the signal due to free probe in solution was measured from the height of the high-field sharp peak of the isotropic component. The percent HTEMPO that was not reduced by ascorbate was determined as the ratio of the membrane-bound peak in the presence of ascorbate to that in its absence, multiplied by 100. Similar measurements were made using the fatty acid spin labels, 5-S-SL and 16-S-SL.

Measurement of antibody binding

nCBS, nGalC, and premixed nCBS-nGalC dispersions, and combined nCBS and nGalC dispersions, were prepared as described above at a final concentration of 1 mg of each lipid per 100 μl H_2O and incubated at 4°C overnight. Antisera to nCBS and anti-GalC were diluted 1/50 with water and 100 μl of either was added to the lipid samples. They were incubated at 4°C for 2 h, diluted to 1 ml with water, centrifuged in an Eppendorf bench centrifuge, the supernatant was removed, and the pellet washed once to remove unbound antibody. Binding of [^{125}I]-anti-Ig to the antibody-bound lipid pellets was determined by resuspending the pellet in 100 μl water and adding 80 μl of [^{125}I]-anti-IgG (diluted 1/50 with water). The samples were incubated 2 h at 4°C, diluted to 1 ml, centrifuged, supernatant removed, and the pellet was washed three times. The pellets were then counted in a Beckman gamma 8000 counter and counts were compared to the total counts in 80 μl [^{125}I]-anti-Ig. Control lipid samples to which [^{125}I]-anti-Ig was added in the absence of anti-CBS or anti-GalC were not centrifuged or washed before addition of [^{125}I]-anti-Ig, but were treated similarly after its addition. Counts from control samples were subtracted from those with anti-CBS or anti-GalC. Separate samples were labeled with [^{14}C]-DPPC and with anti-CBS or anti-GalC in the absence of [^{125}I]-anti-Ig and centrifuged to determine the percent lipid that sedimented in the presence of anti-glycolipid antibody.

RESULTS

FTIR spectroscopy

When HFA-nGalC dispersions were added to C18:0h-CBS dispersions, the FTIR spectra of dry films formed from the lipid suspension indicated that both lipids were affected even in the absence of Ca^{2+}. The frequency of the band due to the antisymmetric double bond O═S—O^- stretching vibration of C18:0h-CBS (Fig. 1, *curve a*) was increased in the presence of HFA-nGalC (Fig. 1, *curve b*, Table 1) indicating that HFA-nGalC caused further dehydration of the sulfate of C18:0h-CBS. Concurrent with the changes in the sulfate vibration, pronounced broadening of bands in the spectra between 1000 and 1200 cm^{-1} arising from the C—O stretching vibrations of galactose oxygens and the sphingosine and fatty acid C—OH groups (Lee et al., 1986) occurred in the spectra of the combined dispersions (Fig. 2, *curve a*). The stretching vibration of C—OH or C—OC groups gave clearly resolved bands at 1145 cm^{-1} for C18:0h-CBS (Fig. 2, *curve d*) and a broader band for HFA-nGalC from 1122 to 1132 cm^{-1} (Fig. 2, *curve c*) but these could not be distinguished in the spectrum of the combined dispersions. The spectrum of the latter is distinctly different from the sum of the HFA-nGalC and C18:0h-CBS spectra in this region (Fig. 2, *curve b*). This indicates that mixing of HFA-nGalC and C18:0h-CBS affects the oxygens in each of the two lipids, probably by altering their hydrogen bonding interactions. However, it is not possible to assign these changes to a specific C—O group.

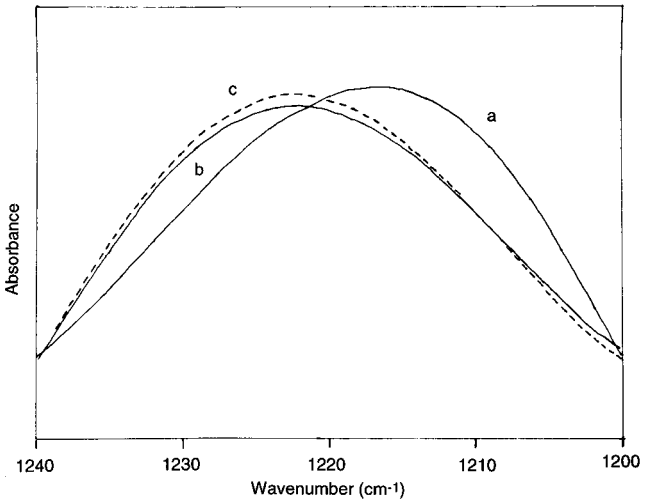

FIGURE 1 Infrared spectra in the sulfate O—S═O antisymmetric stretching vibration region (1200–1240 cm^{-1}) of a dry film of a lipid suspension in water. (*a*) C18:0h-CBS dispersion (*solid line*); (*b*) combined C18:0h-CBS dispersions with HFA-nGalC dispersions (*solid line*); (*c*) premixed C18:0h-CBS–HFA-nGalC dispersion (*dashed line*).

The spectrum of the combined dispersions in the amide I region (Fig. 3, *curve d*) also is distinctly different from the sum of the spectra of the individual lipids (Fig. 3, *curve b*). The low frequency of the major amide I band of HFA-nGalC (Fig. 3, *curve a*), indicating strong intermolecular hydrogen bonding of the amide C═O, and the low frequency of its amide II band (Table 1), indicating involvement of the N—H in a bent intramolecular hydrogen bond, are consistent with the "bent shovel" crystal structure of HFA-GalC (Pascher and Sundell, 1977; Lee et al., 1986). In this conformation, in which the sugar headgroup is bent over and nearly parallel to the bilayer, the amide C═O is involved in intermolecular hydrogen bonding with both the hydroxyl of the sphingosine chain and the 3-OH group of the sugar headgroup of neighboring molecules, while the amide N—H forms a bifurcated intramolecular hydrogen bond with the fatty acid hydroxyl group and the oxygen of the glycosidic linkage. The low frequency of the amide II band of C18:0h-CBS (Table 1) indicates that it has a similar structure (Menikh et al., 1997). However, the higher fre-

TABLE 1 Frequencies of vibrational bands of dry lipid films

Sample	υ(O = S − O$^-$) (cm^{-1})	υ(C − O − S) (cm^{-1})	υ(C − H) (cm^{-1})	υ(C = O)amide I* (cm^{-1})	υ(N − H)amide II (cm^{-1})
C18:0h-CBS	1216	992	2850, 2919	1651, 1626	1541
C18:0h-CBS + Ca^{+2}	1218	990	2851, 2920	1650, 1628, <u>1614</u>	1548
C18:0h-CBS + HFA-nGalC	1223	993	2852, 2920	1658, 1630	1538
C18:0h-CBS + HFA-nGalC + Ca^{+2}	1219	990	2850, 2918	1647, <u>1627</u>	1540
HFA-nGalC			2847, 2916	1650, 1630, <u>1617</u>	1536

*Major band is underlined.

quency of the amide I band of C18:0h-CBS (Fig. 3, *curve c*) relative to that of the major component of HFA-nGalC indicates that the intermolecular hydrogen-bonding interactions of the C═O of C18:0h-CBS are weaker than those of HFA-nGalC.

Combining HFA-nGalC and C18:0h-CBS dispersions caused elimination of the amide I band at 1617 cm^{-1} due to HFA-nGalC and shifted the spectrum of the amide I region of HFA-nGalC, and possibly also C18:0h-CBS, to higher frequencies (Fig. 3, *curve d*). This indicates that the presence of C18:0h-CBS weakens intermolecular hydrogen-bonding interactions of the C═O of HFA-nGalC. The higher frequency of the amide I region of the combined dispersions further indicates dehydration of the amide region of one or both lipids, consistent with the effect of HFA-nGalC on the sulfate of C18:0h-CBS. The amide II band of the combined dispersions was still at a low frequency (Table 1) indicating that the N—H groups of both lipids were still involved in intramolecular hydrogen bonds. The amide A and B bands (Tu, 1982) at 3052 and 3152 cm^{-1} due to C18:0h-CBS (Fig. 4, *curve a*) were absent in the spectrum of the mixture (Fig. 4, *curve d*), confirming a change in environment of the amide group of C18:0h-CBS on addition of HFA-nGalC dispersions.

The hydrocarbon chain conformational order was monitored from the CH_2 symmetric and antisymmetric stretching vibrations. These frequencies were lower for HFA-nGalC than for C18:0h-CBS, indicating the acyl chains of HFA-nGalC are more ordered than those of C18:0h-CBS (Table

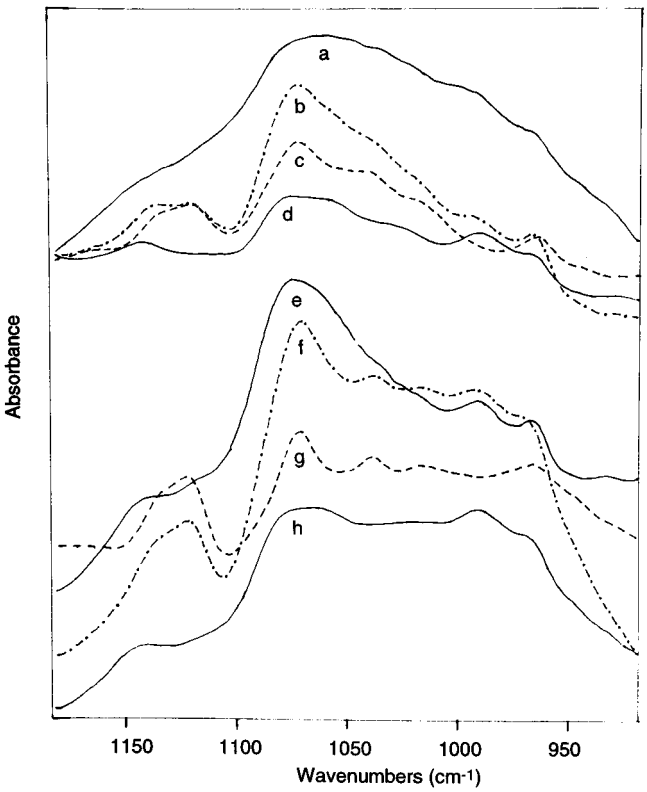

FIGURE 2 Infrared spectra in the C—OH and C—OC stretching vibration region (1000–1200 cm^{-1}). (*a--d*) Dry films prepared from lipid dispersions in water: (*a*) combined C18:0h-CBS and HFA-nGalC dispersions; (*b*) the sum of normalized spectra (*c* and *d*) of HFA-nGalC and C18:0h-CBS dispersions; (*c*) HFA-nGalC; (*d*) C18:0h-CBS. (*e–h*) Dry films prepared from lipid dispersions in 5 mM $CaCl_2$: (*e*) combined C18:0h-CBS and HFA-nGalC dispersions; (*f*) the sum of normalized spectra (*g* and *h*) of HFA-nGalC and C18:0h-CBS dispersions; (*g*) HFA-nGalC; (*h*) C18:0h-CBS. Spectra were normalized according to the intensity of a band at 1340 cm^{-1}.

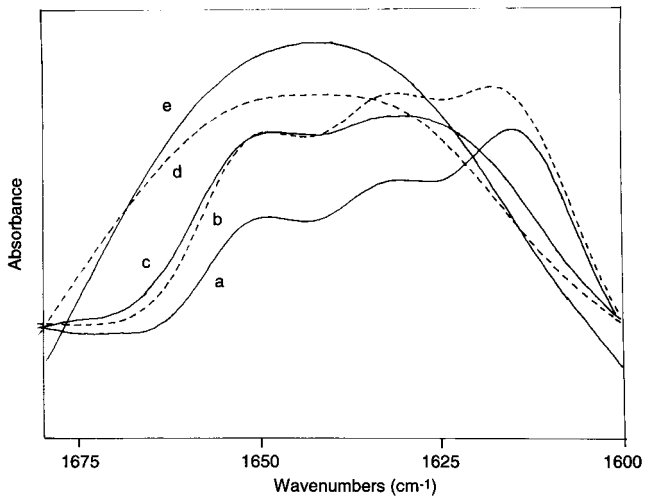

FIGURE 3 Infrared spectra in the amide I C═O stretching region (1600–1700 cm^{-1} of dry films prepared from lipid suspensions in water: (*a*) HFA-nGalC; (*b*) the sum of normalized spectra (*a* and *c*) of HFA-nGalC and C18:0h-CBS dispersions (*dashed line*); (*c*) C18:0h-CBS; (*d*) combined C18:0h-CBS and HFA-nGalC dispersions (*dashed line*); (*e*) premixed C18:0h-CBS-HFA-nGalC dispersions. Spectra were normalized according to the intensity of a band at 1340 cm^{-1}.

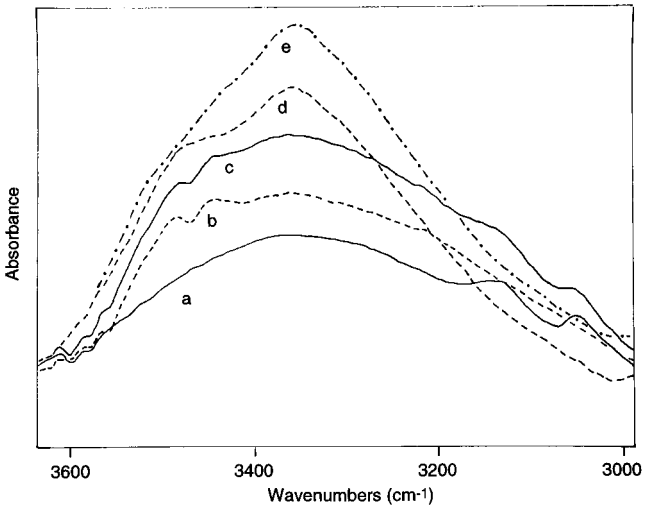

FIGURE 4 Infrared spectra in the O—H stretching vibrational (3200–3500 cm^{-1}) and amide A and B Fermi resonance region (3000–3200 cm^{-1}) of dry films prepared from lipid dispersions in water: (*a*) C18:0h-CBS; (*b*) HFA-nGalC; (*c*) the sum of normalized spectra (*a* and *b*); (*d*) combined C18:0h-CBS–HFA-nGalC dispersions; (*e*) premixed C18:0h-CBS–HFA-nGalC dispersion.

1). This is due to the greater charge repulsion of the C18:0h-CBS headgroup. Mixing of the lipids increased the frequency of the C—H stretching bands to values higher than those of either lipid individually, indicating that mixing disordered the chains of both lipids. This is consistent with the decrease in intermolecular hydrogen bonding interactions of the C═O indicated by the amide I region.

Effect of Ca^{2+} on FTIR spectra

Addition of Ca^{2+} to the combined CBS and GalC dispersions caused a decrease in frequency of the sulfate stretching vibration, resulting in a similar frequency as for C18:0h-CBS plus Ca^{2+} by itself (Table 1), indicating that Ca^{2+} binds to the dehydrated sulfate in the lipid mixture. Moreover, Ca^{2+} also decreased the frequency of the stretching vibration of the C—O group linking the sulfate to the sugar headgroup of C18:0h-CBS in the combined dispersions (Table 1) with a significant decrease in its bandwidth (not shown). Ca^{2+} had a similar effect on C—O—S of C18:0h-CBS alone (Table 1) (Menikh et al., 1997). Thus the presence of HFA-nGalC does not prevent interaction of Ca^{2+} with the sulfate of C18:0h-CBS.

In the presence of Ca^{2+}, the band due to the stretching vibration of C—OH and C—OC groups for the combined dispersions was at ~1147 cm^{-1} (Fig. 2, *curve e*) and resembled that of the Ca^{2+} salt of C18:0h-CBS (Fig. 2, *curve h*). The broader band of HFA-nGalC at a lower frequency (Fig. 2, *curve g*) does not contribute as significantly to the spectrum of the combined dispersions (Fig. 2, *curve e*) as indicated by comparison with the sum of the spectra of the two lipids (Fig. 2, *curve f*). This indicates that in the presence of Ca^{2+}, C18:0h-CBS affects the oxygens of HFA-nGalC, but those of C18:0h-CBS are little affected by HFA-nGalC. Because Ca^{2+} clearly interacts with C18:0h-CBS in the mixture, and since the oxygens of HFA-nGalC are still affected by the presence of Ca^{2+}-CBS, a ternary complex of Ca^{2+} with HFA-nGalC and C18:0h-CBS must be present, although it cannot be deduced whether Ca^{2+} interacts jointly with C18:0h-CBS and HFA-nGalC in the complex, or only with the C18:0h-CBS.

Ca^{2+} decreased the frequency of the predominant amide I band of C18:0h-CBS by itself (Fig. 5, *curve a*) and increased that of the amide II band (Table 1) (Menikh et al., 1997). This indicates a rearrangement of the hydrogen-bonding network of C18:0h-CBS to one in which linear intermolecular hydrogen-bonding of the N—H with the C═O of a neighboring lipid molecule predominates. The bent shovel conformation may be destabilized, resulting in a conformational change to an extended conformation in which the sugar headgroup is nearly perpendicular to the bilayer (Menikh et al., 1997). However, in the spectrum of the combined dispersions, the predominant amide I band was at a higher frequency (Fig. 5, *curve d*) than those of the individual lipids (compare with the summed spectra, Fig. 5, *curve c*) and the predominant amide II band was only a little greater than that of the combined dispersions without Ca^{2+} (Table 1), indicating that Ca^{2+} induced much less rearrangement of the hydrogen-bonding network of the lipids in the combined dispersions than of C18:0h-CBS by itself. Thus interaction of HFA-nGalC and C18:0h-CBS in the combined dispersions in the presence of Ca^{2+} decreased the

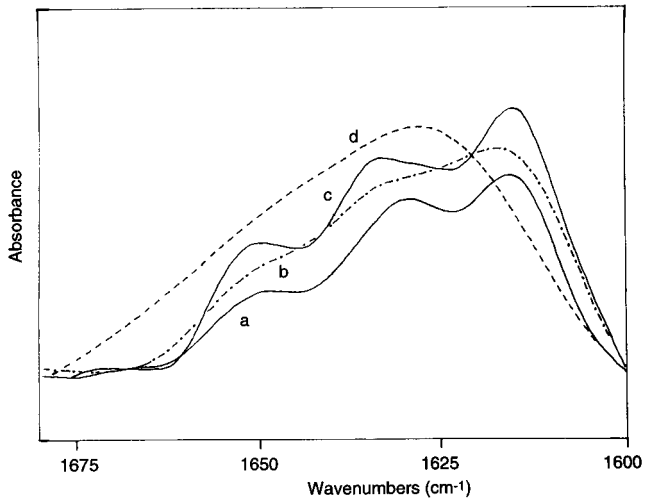

FIGURE 5 Infrared spectra in the amide I C═O stretching region (1600–1700 cm^{-1} of dry films prepared from lipid suspensions in 0.5 mM $CaCl_2$: (*a*) C18:0h-CBS; (*b*) HFA-nGalC (*dash-dot*); (*c*) the sum of normalized spectra (*a* and *b*) of HFA-nGalC and C18:0h-CBS dispersions; (*d*) combined C18:0h-CBS and HFA-nGalC dispersions (*dashed line*). Spectra were normalized according to the intensity of a band at 1340 cm^{-1}.

hydrogen-bonding interactions of the C═O of one or both lipids, as in the absence of Ca^{2+}. Furthermore, the interaction decreased the extent of the Ca^{2+}-induced rearrangement of the hydrogen-bonding of the N—H of CBS from intramolecular to intermolecular. However, Ca^{2+} caused some increase in participation of the C═O of one or both lipids in hydrogen bonding, since the frequency of the lowest frequency amide I band of the combined dispersions decreased from 1630 to 1627 cm^{-1} on addition of Ca^{2+}.

Ca^{2+} decreased the frequencies of the CH_2 symmetric and antisymmetric stretching vibrations of the lipids in the combined dispersions, indicating that it increased conformational order, also consistent with the increased participation of the C═O in hydrogen bonding. The effect of Ca^{2+} on the C—H stretching bands of the lipid mixture differs from its effect on pure C18:0h-CBS where it had a small disordering effect (Table 1).

The FTIR spectra indicated that most of the HFA-nGalC and C18:0h-CBS in the combined dispersions in the absence of Ca^{2+} was affected by the interaction even though the dispersions of each lipid probably consisted of multilayered microstructures. The spectrum of a sample where the two lipids were premixed together in solvent before dispersion in water closely resembles that of the combined HFA-nGalC and C18:0h-CBS dispersions (Compare Fig. 1, *curves b* and *c*, Fig. 3, *curves d* and *e*, and Fig. 4, *curves d* and *e*). Although the spectra in the presence of Ca^{2+} indicate that combining the two sets of dispersions clearly affects one or both lipids, the proportion of the lipid affected was less clear (e.g., compare Fig. 5, *curves c* and *d*) than in the absence of Ca^{2+}.

The films used for the FTIR spectra above were prepared by drying an aliquot of the suspension on a CaF_2 plate or by sedimenting the lipid, smearing the pellet on the plate, and drying the film. Similar results were obtained if the pellet was not dried. However, if the dispersions were not pelleted but were examined as dilute suspensions at a concentration of 0.5 mg/ml, combining the GalC and C18:0h-CBS dispersions had no effect on the sulfate band of C18:0h-CBS, indicating that little interaction occurred in the absence of Ca^{2+} (not shown). Thus the suspensions must be very concentrated in order for an interaction between GalC and CBS microstructures to occur in the absence of Ca^{2+}.

Sedimentation of CBS and GalC

This was confirmed by combining suspensions of nCBS and nGalC containing [^{14}C]-DPPC and measuring the amount of lipid that could be sedimented by centrifugation. (Natural mixtures of GalC and CBS were used for the rest of the experiments because of their lower cost.) In the absence of salt, nCBS does not sediment well, while almost 100% of nGalC sediments (Table 2). If labeled nCBS dispersions were added to unlabeled nGalC dispersions, the amount of nCBS that sedimented along with the nGalC increased relative to nCBS alone. The amount of nCBS that sedimented with the nGalC increased with increase in the lipid concentration. If the water in the sample was evaporated, as was done with the FTIR samples, and then the sample was rehydrated and resuspended in water, even more of the nCBS sedimented with the nGalC on centrifugation (Table 2, set 2). Almost all of the nGalC still sedimented even after this greater interaction with nCBS. These results indicate that the nCBS and nGalC microstructures interact, and the interaction increases with lipid concentration and/or evaporation of the water. Dispersions of premixed nGalC and nCBS did not sediment well (Table 2, set 1), indicating the premixed lipid behaved more like nCBS than nGalC. Thus premixing with nCBS caused flotation of nGalC. Sedimentation increased with increasing amounts of nGalC in the mixed suspensions. This suggests that the microstructures obtained when nCBS dispersions interact with nGalC dispersions differ from those obtained by premixing the lipids.

TABLE 2 Amount of lipid sedimented by centrifugation

Sample	% Lipid in pellet	
	High Concentration*	Low Concentration†
Set 1		
CBS	6.0 ± 2.2 (n = 3)	6.9 ± 4.5 (n = 4)
GalC	93.1 ± 4.6 (n = 3)	98.8 (n = 1)
CBS‡ + GalC	23.2 ± 2.6 (n = 2)	9.6 ± 2.3 (n = 6)
CBS + GalC‡	95.2 ± 3.4 (n = 2)	97.2 (n = 1)
Premixed CBS-GalC (1:1)	15.8 (n = 1)	18.8 ± 9.8 (n = 2)
Premixed CBS-GalC (1:2)	30.2 (n = 1)	
Premixed CBS-GalC (1:3)	38.0 (n = 1)	
Set 2		
CBS‡ + GalC	25.8	
CBS + GalC‡	91.9	
CBS‡ + GalC after evaporation§	49.4	
CBS + GalC‡ after evaporation§	96.5	

Labeled with [^{14}C]-DPPC; n, number of experiments.
*10 mg CBS/ml.
†0.5–1/mg CBS/ml.
‡Indicates which lipid dispersion contained [^{14}C]-DPPC for combined dispersions.
§Water was evaporated to mimic treatment for FTIR spectroscopy, lipid was rehydrated and redispersed in same volume of water before centrifugation.

Resonance energy transfer between fluorescent probes

A *trans* interaction between GalC and CBS was expected to affect only the lipid on the outer surface of the microstructures, and not the lipid in inner lamellae. The FTIR results indicating that most of the lipid, both CBS and GalC, is affected by combining these lipid dispersions suggested that the GalC and CBS microstructures were either single-layered or they might have fused with each other. Fluorescent probes were used in an attempt to determine whether fusion

of the lipid microstructures and mixing of the two lipids had occurred (Hoekstra and Duzgunes, 1993). Some quenching of the probes occurred on incorporation in GalC, indicating poor solubility in this lipid. Thus the probes had limited usefulness for studying these lipids, but nevertheless provided some evidence that interaction between these lipid microstructures occurred. NBD-PE and Rho-PE were added to nCBS dispersions, and these were combined with unlabeled nGalC dispersions. The increase in intensity of the NBD donor emission fluorescence at 530 nm, due to decreased resonance energy transfer between NBD and Rho upon dilution into the unlabeled dispersions, was compared to the NBD fluorescence after solubilizing the lipid in TX-100. If nCBS dispersions containing these probes were added to nGalC dispersions in a 1:1 mole ratio there was only a small increase in fluorescence, indicating little dilution of the probe into nGalC had occurred (Table 3, set 1, line 3 versus lines 1 and 2). However, if nCBS, nGalC, and the probes were premixed in solvent before preparation of the dispersions (line 4), there was also no increase in fluorescence relative to nCBS alone, indicating that the probes did not partition into nGalC in the presence of nCBS or were clustered in the nCBS-nGalC mixture. In fact, the fluorescence of the nCBS-nGalC mixture actually decreased relative to nCBS alone, indicating that the premixed nCBS-nGalC had properties between those of nCBS and nGalC, causing decreased solubility of the probe, increased probe clustering, and greater quenching or greater energy transfer to Rho compared to nCBS alone. This decreased solubility of the probes in nGalC or mixed nCBS-nGalC dispersions made it difficult to determine whether fusion and mixing of the lipids occurred on combining nCBS dispersions with nGalC dispersions.

However, if nCBS dispersions containing the probes were combined with nCBS dispersions lacking the probes together with nGalC dispersions also lacking the probes, in a mole ratio of labeled nCBS to unlabeled nCBS to nGalC of 1:4:5, some increase in fluorescence, indicating dilution of the probes, occurred even at a low lipid concentration

TABLE 3 Mixing of CBS and GalC monitored from increased fluorescence of NBD-PE due to decreased energy transfer to Rho-PE on dilution of probes

Line	Sample	Final probe concentration in lipid if mixing occurred (mol %)*	Emission (530 nm)		% Dilution relative to TX-100‡	Mean % dilution relative to TX-100§
			H_2O	TX-100†		
			Set 1			
1	CBS	0.8	3.6 ± 0.1	36.8 ± 2.5		0
2	2x CBS	0.4	10.0 ± 0.3	38.6 ± 0.8		16.4 ± 0.2
3	CBS¶ + GalC (1:1)	0.4	4.5 ± 0.8	32.6 ± 0.3		3.4 ± 1.5
4	premixed CBS-GalC (1:1)	0.4	3.2 ± 0.2	37.4 ± 0.1		0 (n = 3)
			Set 2			
	Original suspension					
5	CBS	0.8	1.5	15.0	0	0
6	CBS¶ + CBS (1:4)	0.16	1.5	14.9	0	0
7	CBS¶ + CBS + GalC (1:4:5)	0.08	2.3	20.0	1.3	2.7 ± 1.5 (n = 5)
After centrifugation and resuspension of pellet in supernatant						
8	CBS¶ + CBS (1:4)	0.16	1.6	14.0	1.2	0.6 ± 0.6
9	CBS¶ + CBS + GalC (1:4:5)	0.08	2.4	15.6	5.5	4.3 ± 1.2 (n = 2)
After centrifugation and resuspension of pellet in fresh water						
10	CBS¶ + CBS (1:4)‖	0.16	0.12	0.76	6.1	1.5 ± 3.0
11	CBS¶ + CBS + GalC (1:4:5)**	0.08	0.75	1.44	42.4	30.7 ± 8.9 (n = 4)
			Set 3			
12	CBS	0.8	2.3	20.6	0	
13	CBS¶ + CBS (1:4)	0.16	3.4	21.6	4.2	
14	CBS¶ + CBS + GalC (1:4:5)	0.08	7.2	28.4	14.2	

In set 1, labeled CBS suspensions were combined with unlabeled GalC suspensions in a 1:1 mol ratio. In set 2, labeled CBS suspensions were combined with unlabeled CBS suspensions in a 1:4 mol ratio, which were then combined with unlabeled GalC suspensions in a 1:1 CBS/GalC mol ratio to allow greater probe dilution on mixing and to permit detection of probe dilution into CBS even if the probe did not partition into GalC or the CBS-GalC mixture. All samples in sets 1 and 2 were at a low lipid concentration of 0.5–1 mg CBS/ml, while that for set 3 was at a high lipid concentration of 10 mg CBS/ml during the incubation stage (they were then diluted for measurement).

*The same amounts of probes were used in all samples in a set. Probe concentration in the lipid is varied by varying the amount of total lipid.

†Corrected for effect of TX-100 on quantum yield of NBD-PE.

‡Percent dilution is determined from emission of suspension in water divided by emission in TX-100, times 100. The value obtained for CBS was subtracted. Thus, emission in TX-100 corresponds to 100% dilution, and in CBS corresponds to 0% dilution.

§For set 1, data from three different experiments are averaged. For set 2, data from a representative experiment are shown and mean values ±SD of percent dilution from five different experiments is also given.

¶Indicates which dispersion was labeled with fluorescent probes for combined dispersions.

‖The pellet contained only 5% CBS; 95% CBS and probes were removed in the supernatant. This is reflected by the reduced emission in TX-100.

**Pellet contained only 8.2% CBS.

(Table 3, set 2, line 7 versus line 6). No dilution of the probes into unlabeled CBS occurred if nGalC dispersions were omitted (line 6 versus line 5). Sedimentation of the lipid and examination of the fluorescence of the sedimented lipid (after resuspension in fresh water) revealed a significant decrease in energy transfer, indicating probe dilution had occurred in the sedimented fraction (line 11 versus line 10). However, this fraction contained only 8% of the nCBS and probes. Since the interaction between [^{14}C]-labeled CBS and GalC microstructures increased with lipid concentration, the interaction of fluorescent probe-labeled dispersions was also measured at a higher lipid concentration (Table 3, set 3). At this higher concentration, a greater increase in fluorescence occurred on mixing of labeled nCBS dispersions, unlabeled nCBS dispersions, and unlabeled nGalC dispersions (line 14 versus line 13). The results for set 1 indicate that the probes must have become diluted primarily into the unlabeled nCBS and not into the nGalC. Thus the experiments in Table 3 indicate that mixing of labeled and unlabeled nCBS dispersions occurred in the presence of nGalC dispersions, but do not reveal whether the nGalC and nCBS also became mixed. However, the requirement for the presence of nGalC dispersions for this mixing of unlabeled and labeled nCBS indicates that some kind of interaction between the nCBS and nGalC microstructures must have occurred.

Accessibility of HTEMPO to ascorbate in the external aqueous phase

In order to obtain some information about the structure of the lipid dispersions before and after interaction with each other, they were labeled with the acyl ammonium spin-label HTEMPO and the accessibility of the spin label to reduction by ascorbate was determined. Ascorbate is a relatively nonpermeant reducing agent that reduces the nitroxide spin label resulting in signal loss (Kornberg and McConnell, 1971). Since this spin label is mostly membrane-bound (except in nGalC, vide infra) with its spin-label group exposed at the surface of the bilayer, ascorbate should reduce only the HTEMPO exposed on the surface of the lipid microstructures and free HTEMPO in the external aqueous phase, if the microstructures are sealed. This spin label has been used to obtain an estimate of the outer surface exposure and degree of multilamellarity of multilayered vesicles (Stewart and Boggs, 1990). Ascorbate caused reduction of 20% of membrane-bound HTEMPO in nCBS, a little more than found for egg PC, suggesting that the nCBS formed sealed, multilayered vesicles (Table 4, column 1). Only ~50% of membrane-bound HTEMPO was protected from reduction in nGalC. The spin label was much less soluble in nGalC than in nCBS, as revealed by a larger isotropic signal due to spin label free in solution (Table 4, column 2). The greater reduction in nGalC could have been due to rapid exchange between free and bound spin label or to formation of structures open to the aqueous phase. GalC has been reported to form a variety of structures, including lamellar nanotubes, when suspended in water (Archibald and Mann, 1994; Kulkarni et al., 1995).

The external free HTEMPO was also reduced by ascorbate (Table 4, column 3); 48% of the free spin label was protected from reduction in nCBS (compared to 66% for egg PC), supporting the conclusion that the nCBS forms sealed vesicles. Although much more free HTEMPO was present for nGalC dispersions, only 5% was protected from reduction, further suggesting that either the microstructures formed by nGalC were not sealed, or they did not entrap much aqueous phase. Premixed nCBS-nGalC dispersions bound much more of the HTEMPO than nGalC, but they also protected only a small amount of the probe, suggesting that they also did not form sealed structures or did not entrap much aqueous phase.

Interestingly, if HTEMPO-labeled nCBS dispersions were combined with unlabeled nGalC dispersions, 100% of both membrane-bound and free spin label became accessible to ascorbate and was completely reduced (Table 4). However, if HTEMPO-labeled nGalC dispersions were combined with unlabeled nCBS dispersions, the probe was not any more accessible to ascorbate than when in nGalC dispersions alone. The amount of free probe was much less than in GalC alone, but 22% was protected from reduction,

TABLE 4 Protection of membrane-bound and free HTEMPO from reduction by ascorbate

	% Membrane-bound HTEMPO left unreduced*	Relative amount of free HTEMPO†	% Free HTEMPO left unreduced†
egg PC	86.7		65.9
CBS	79.5 ± 5.2	7.6 ± 1.4	47.9 ± 7.8
GalC	53.1 ± 7.2	38.2 ± 4.6	5.0 ± 0.6
CBS‡ + GalC	0 ± 0	6.9 ± 0.8	0 ± 0
CBS + GalC‡	58.9 ± 14	9.2 ± 3.6	21.6 ± 8.4
Premixed CBS-GalC	12.2 ± 8.4	11.5 ± 3.1	5.5 ± 4.0

Mean of four experiments ±SD except for egg PC.
*Measured from height of low-field membrane bound peak.
†Measured from height of high-field aqueous peak.
‡Indicates which lipid dispersion is labeled with HTEMPO for combined dispersions.

indicating that some probe was trapped in the new structures formed and that the structures were sealed. Fatty acid spin labels with the nitroxide group on carbon 5 or 16, in the hydrocarbon region of the bilayer, in either nCBS or nGalC, remained inaccessible to ascorbate when the dispersions were combined (not shown). These results indicate that when nCBS microstructures interact with nGalC microstructures, the nCBS microstructures are completely disrupted, but the nGalC ones are not. However, the hydrocarbon chains remain unexposed to ascorbate, indicating that in the final structure the acyl chains are still sequestered from water. When nCBS, nGalC, and HTEMPO were premixed in solvent before dispersion of the lipid, the membrane-bound probe was also very accessible to ascorbate, although not as completely accessible as when the two sets of dispersions were combined.

The following results indicate that some of the nCBS interacts with nGalC: 1) the protection of the probe when initially located in the nGalC dispersions and complete accessibility when initially located in the nCBS dispersions when the two sets of dispersions are combined; 2) the fluorescence results indicating mixing of the labeled and unlabeled nCBS microstructures in the presence of nGalC; and 3) the sedimentation results indicating cosedimentation of some of the nCBS with nGalC when nCBS and nGalC dispersions are combined. These results suggest the following phenomenon: the nCBS multilayered microstructures interact with the outer layer of the nGalC microstructures and are then disrupted, allowing release of free HTEMPO and causing the nCBS to fuse into a single bilayer surrounding each nGalC microstructure. The fact that all free HTEMPO is released suggests that all of the CBS microstructures participate initially in this interaction. The fact that all membrane-bound HTEMPO becomes accessible to ascorbate further suggests that all of the CBS multilayered microstructures fuse into single-layered microstructures, although the sedimentation results indicate that they do not all remain associated with GalC. All of the CBS probably cannot be accommodated in a single layer surrounding the GalC microstructures and thus form separate CBS single-layered microstructures. Because the nCBS microstructures are now single-layered, both lipid-bound and free HTEMPO are much more accessible to ascorbate. If the nCBS microstructures had fused with the nGalC microstructures such that nCBS and nGalC became mixed in the same bilayer, this should have led to an nCBS-nGalC mixture in which HTEMPO is accessible to ascorbate regardless of whether it was initially in the nCBS or in the nGalC dispersions. It should also have led to flotation of the nGalC, which did not occur. Rather, interaction of the nCBS with the nGalC caused sedimentation of the nCBS. The amount of CBS that sedimented with GalC increased after evaporation and resuspension of the lipid. This may allow more of the nCBS microstructures to fuse around the nGalC microstructures, possibly due to disruption and reformation of the nGalC microstructures, thus exposing more of the total nGalC surfaces for interaction with the nCBS.

Accessibility of lipids to anti-GalC and anti-CBS antibodies

Interaction of nCBS with nGalC as proposed above should sequester nGalC from the aqueous phase, as suggested by the protection of HTEMPO, which was initially in GalC from ascorbate reduction. This was confirmed using anti-GalC and anti-CBS antibodies. The primary antibody-lipid complexes were pelleted, allowing removal of unbound primary antibody, and binding of [^{125}I]-anti-Ig to the resuspended primary antibody-lipid complexes was measured. Use of [^{14}C]-DPPC labeled dispersions showed that the amount of lipid that sedimented in the presence of primary antibody (Table 5) was similar to that in its absence (Table 2) except for the premixed nGalC-nCBS dispersions, which sedimented much more in the presence of either anti-CBS or anti-GalC antibodies than without antibodies. When nCBS dispersions were combined with nGalC dispersions, binding of [^{125}I]-anti-Ig following anti-GalC was greatly decreased compared to nGalC alone, even though the amount of nGalC in the pellet was similar in both cases (Table 5). This indicated that nGalC was sequestered from the anti-GalC. However, binding of [^{125}I]-anti-Ig following anti-CBS increased relative to nCBS alone. This increased binding is due to the greater amount of nCBS in the pellet in the presence of nGalC dispersions, but indicates the nCBS was

TABLE 5 Sedimentation of lipid and amount of anti-CBS and anti-GalC antibodies bound to lipid pellet

Sample	% Lipid in pellet*	% [^{125}I]-anti-Ig bound†	
		Expt. I‡	Expt. II
GalC + anti-GalC	98.7	21.4 ± 1.4	32.3
GalC + anti-CBS	99.3	2.3 ± 0.5	
CBS + anti-GalC	0	3.8 ± 0.9	6.2
CBS + anti-CBS	3.9	5.7 ± 1.3	
GalC§ + CBS + anti-GalC	95.5	6.8 ± 1.6	10.8
GalC + CBS§ + anti-GalC	13.7		
GalC§ + CBS + anti-CBS	94.9	11.3 ± 1.5	
GalC + CBS§ + anti-CBS	6.8		
Premixed CBS-GalC + anti-GalC	69.2	13.4 ± 0.6	23.9
Premixed CBS-GalC + anti-CBS	65.7	15.4 ± 0.7	

*Determined from lipid dispersions containing [^{14}C]-DPPC. Anti-Ig was not added. For combined GalC and CBS dispersions the [^{14}C]-DPPC was included in the GalC dispersion for one sample and in the CBS dispersion for another sample.

†Determined from binding of [^{125}I]-anti-Ig to lipid dispersions without [^{14}C]-DPPC, expressed as percent of total anti-Ig added that was found in the pellet. Binding of [^{125}I]-anti-Ig to the dispersions in the absence of anti-CBS or anti-GalC Ab has been subtracted.

‡Done in duplicate. Mean range is shown.

§Indicates which dispersion was labeled with [^{14}C]-DPPC for combined dispersions in the absence of [^{125}I]-anti-Ig.

still accessible to anti-CBS. Binding of [^{125}I]-anti-Ig to the premixed nCBS-nGalC dispersions was relatively high following both anti-CBS and anti-GalC antibodies; the amount of binding was consistent with the amount of lipid in the pellet. Thus, when CBS dispersions were combined with GalC dispersions, the resulting structure of the sedimentable lipid exposed CBS to the aqueous phase but sequestered GalC. When the lipids were premixed, they formed a structure in which both CBS and GalC were accessible to the aqueous phase. This supports the conclusion that when CBS dispersions are added to GalC dispersions they form a CBS bilayer surrounding the nGalC structures. In these structures, the CBS must interact with the GalC via *trans* interactions between the apposed bilayers.

DISCUSSION

The results of the FTIR, sedimentation, resonance energy transfer, and HTEMPO accessibility studies all indicate that CBS microstructures strongly interact with GalC microstructures in water even in the absence of Ca^{2+}. Previous vesicle aggregation studies with DMPC/cholesterol vesicles containing 10–20 mol % GalC or CBS (Stewart and Boggs, 1993) and ESI-MS studies of oligomeric interactions between GalC and CBS in methanol (Koshy and Boggs, 1996) indicated that divalent cations were necessary for interaction to occur. The greater glycolipid surface density and multivalency of these pure glycolipid microstructures may be responsible for their strong interaction in the absence of Ca^{2+}. The HTEMPO accessibility and antibody binding studies further suggest that the CBS forms a single layer surrounding the GalC microstructures, thus sequestering the GalC from ascorbate and antibody added to the external aqueous phase. CBS and GalC would thus interact via *trans* interactions across apposed bilayers in such structures.

The resultant GalC-CBS microstructures formed by combining GalC and CBS dispersions differ in some respects from those formed by premixing GalC and CBS in organic solvent before dispersion of the dry lipid in water. The former are denser, can be sedimented more easily, and do not bind anti-GalC, while the latter do. However, they are similar with regard to the lack of dilution of fluorescent probes relative to CBS alone and the extensive reduction (complete in the former case and nearly complete for the latter) of HTEMPO that occurs on addition of ascorbate. It is not known whether premixing of GalC and CBS results in mixing of the two lipids in the same bilayer, where lateral *cis* interactions could occur, or in the same type of structure obtained on combining GalC and CBS dispersions. The reduced density suggests the former since repulsion between bilayers all containing a significant amount of CBS would cause greater water entrapment and reduced multilamellarity, and thus more similar behavior to that of CBS alone. This is also consistent with the reactivity with both anti-CBS and anti-GalC antibodies. However, the more complete reduction of HTEMPO compared to CBS alone indicates that if the lipids are mixed laterally, the structures are either single-layered or not sealed. The lack of dilution of fluorescent probes could be due to the greater order of the mixed GalC-CBS bilayer causing it to behave more like GalC alone, or it could indicate phase separation of the CBS and GalC, possibly as in the structures formed by combining GalC and CBS dispersions.

GalC and CBS have been observed by microscopic techniques to form a variety of structures when dispersed in water, including multilamellar vesicles, long unilamellar or multilamellar cylinders, chochleate cylinders, and helical lamellar ribbons, depending partly on the method of preparation and subsequent treatment of the dispersions and on the molecular species of the lipid used (Archibald and Mann, 1994; Kulkarni et al., 1995, 1999; Curatolo and Neuringer, 1986; Goldstein et al., 1997). Mg^{2+} had a significant effect on GalC microstructures, indicating interaction of this divalent cation with GalC alone (Goux et al., 1995). The structure of premixed GalC-CBS dispersions has been reported in only one study, and this was in glycol. HFA-nGalC-CBS mixtures formed mainly cochleate cylinders, and NFA-nGalC-CBS mixtures formed mainly unilamellar cylinders in glycol (Archibald and Mann, 1994). At low concentrations CBS was incorporated into the HFA-nGalC cylinders, but at high concentrations it formed CBS-enriched blebs and lamellar phases attached to the end of the cylinders. Incorporation of CBS in NFA-nGalC inhibited its formation of helical structures.

The FTIR spectra of premixed dispersions were similar to the spectra of the structures resulting from addition of CBS dispersions to GalC dispersions. If CBS and GalC are laterally mixed in the premixed dispersions they could interact by lateral *cis* interactions. *Trans* interactions between apposed bilayers containing both GalC and CBS are unlikely in the absence of salt due to charge repulsion. The FTIR spectra indicate that interactions between these lipids in premixed dispersions have a similar effect on the lipids as *trans* interactions between apposed GalC and CBS bilayers in the structures resulting from adding CBS dispersions to GalC dispersions. These effects are dehydration of the sulfate, changes in the hydrogen bonding interactions of the sugar and other oxygens, decreased intermolecular hydrogen bonding of the amide C═O of GalC and dehydration of the amide region of one or both of the lipids in the mixture, and disordering of the acyl and sphingosine chains of both lipids. Although GalC molecules also interact laterally with each other in bilayers by intermolecular hydrogen-bonding, and the same is true for CBS, resulting in high phase transition temperatures for these glycolipids, the FTIR results indicate that heterotypic lateral interactions between GalC and CBS molecules are different from the homotypic interactions between these lipids.

The spectra also indicate that Ca^{2+} interacts with the sulfate of CBS. Although they do not reveal which other groups of CBS and GalC interact with Ca^{2+} or which groups participate in the interaction between the two lipids, they do show that the sulfate is not directly involved in interaction with GalC, since it can still bind to Ca^{2+}. In the presence of Ca^{2+}, CBS affected the oxygens of GalC, but GalC had little effect on those of the Ca^{2+}-CBS complex. This indicates that a ternary complex of Ca^{2+} with GalC and CBS must be present but does not reveal whether Ca^{2+} interacts jointly with CBS and GalC in the complex or only with the CBS. Ca^{2+} did not have as great an effect on the amide region of CBS in the presence of GalC as we reported earlier for CBS alone (Menikh et al., 1997); it increased the linear hydrogen-bonding of the C═O and N—H of one or both lipids in the combined dispersions, but not to the extent that it does for CBS alone or that which occurs for GalC alone. Thus Ca^{2+} did not cause rearrangement of the hydrogen-bonding network of CBS. This suggests that the "bent shovel" conformation of CBS may be retained in the combined dispersions with GalC and Ca^{2+}. Inhibition of a Ca^{2+}-induced conformational change of the sugar headgroup of CBS to an extended conformation by the presence of GalC may indicate that the *trans* interactions between these two lipid headgroups occur between the sugars in their bent-over, bilayer parallel conformations. However, Ca^{2+} increased the conformational order of the lipid chains in the combined dispersions, perhaps due to the small increase in hydrogen-bonding of the amide region of the lipids.

In myelin, GalC and CBS would be 38 mol % of the lipid on the extracellular surface (Inouye and Kirschner, 1988). The pronounced interactions found here between pure GalC and pure CBS dispersions, even in the absence of Ca^{2+}, and the weaker interactions found earlier between DMPC/cholesterol liposomes containing 10–20 mol % of GalC with similar liposomes containing CBS in the presence of divalent cations, suggest that *trans* interactions between these glycolipids on the apposed myelin surfaces could occur if they are not prevented by steric hindrance due to transmembrane proteins such as the proteolipid protein or protein zero, which protrude above the extracellular myelin surface (Kirschner and Blaurock, 1992). These proteins may have a heterogeneous distribution under some conditions, which could then allow adhesion of protein-free regions of the myelin surfaces. Indeed, Ca^{2+} has been found to decrease the interlamellar separation in myelin resulting in a dehydrated structure, with lateral segregation of intramembranous particles, probably due to transmembrane proteins, out of the closely packed domains (Melchior et al., 1979; Hollingshead et al., 1981). *Trans* glycolipid-glycolipid interactions might also cause signal transmission across the membrane similar to the effects of anti-GalC and anti-CBS antibodies on cultured oligodendrocytes (Benjamins and Dyer, 1990; Bansal et al., 1988). Lateral *cis* interactions between these two lipids could also occur in myelin. The FTIR results on premixed dispersions indicate that *cis* interactions would also dehydrate the headgroup and amide interfacial region. This would contribute to the stability of the bilayer in myelin.

This study was supported by the Multiple Sclerosis Society of Canada through a postdoctoral fellowship (to A.M.) and a grant from the Medical Research Council of Canada (to J.M.B.).

REFERENCES

Archibald, D. D., and S. Mann. 1994. Self-assembled microstructures from 1,2-ethanediol suspensions of pure and binary mixtures of neutral and acidic biological galactosylceramides. *Chem. Phys. Lipids.* 69:51–64.

Bansal, R., A. L. Gard, and S. E. Pfeiffer. 1988. Stimulation of oligodendrocyte differentiation in culture by growth in the presence of a monoclonal antibody to sulfated glycolipid. *J. Neurosci. Res.* 21:260–267.

Benjamins, J. A., and C. A. Dyer. 1990. Glycolipids and transmembrane signaling in oligodendroglia. *Ann. NY Acad. Sci.* 605:90–100.

Boggs, J. M., K. M. Koshy, and G. Rangaraj. 1988. Influence of structural modifications on the phase behavior of semi-synthetic cerebroside sulfate. *Biochim. Biophys. Acta.* 938:361–372.

Crook, S. J., R. Stewart, J. M. Boggs, A. I. Vistnes, and B. Zalc. 1987. Characterization of anti-cerebroside sulfate antisera using a theoretical model to analyse liposome immune lysis data. *Mol. Immunol.* 24: 1135–1143.

Curatolo, W., and L. J. Neuringer. 1986. The effects of cerebrosides on model membrane shape. *J. Biol. Chem.* 261:17177–17182.

Eggens, I., B. Fenderson, T. Toyokuni, B. Dean, M. Stroud, and S. Hakomori. 1989. Specific interaction between Le^x and Le^x determinants. A possible basis for cell recognition in preimplantation embryos and in embryonal carcinoma cells. *J. Biol. Chem.* 264:9476–9484.

Goldstein, A. S., A. N. Lukyanov, P. A. Carlson, P. Yager, and M. H. Gelb. 1997. Formation of high axial ratio microstructures from natural and synthetic sphingolipids. *Chem. Phys. Lipids.* 88:21–36.

Goux, W. J., H. Smith, and D. R. Sparkman. 1995. Assembly of Alzheimer-like, insoluble filaments from brain cerebrosides. *Neurosci. Lett.* 192:149–152.

Hakomori, S.-I. 1984. Tumor-associated carbohydrate antigens. *Annu. Rev. Immunol.* 2:103–126.

Hakomori, S.-I. 1991. Carbohydrate-carbohydrate interaction as an initial step in cell recognition. *Pure Appl. Chem.* 63:473–482.

Hoekstra, D., and N. Duzgunes. 1993. Lipid mixing assays to determine fusion in liposome systems. *Methods Enzymol.* 220:15–32.

Hollingshead, C. J., D. L. D. Caspar, V. Melchior, and D. A. Kirschner. 1981. Compaction and particle segregation in myelin membrane arrays. *J. Cell Biol.* 89:631–644.

Inouye, H., and D. A. Kirschner. 1988. Membrane interactions in nerve myelin. II. Determination of surface charge from biochemical data. *Biophys. J.* 53:247–260.

Kirschner, D. A., and A. E. Blaurock. 1992. Organization, phylogenetic variations, and dynamic transitions of myelin. *In* Myelin: Biology and Chemistry. R. E. Martenson, editor. CRC Press, Boca Raton, FL. 1–78.

Kornberg, R. D., and H. M. McConnell. 1971. Inside-outside transitions of phospholipids in vesicle membranes. *Biochemistry.* 10:1111–1120.

Koshy, K. M., and J. M. Boggs. 1983. Partial synthesis and physical properties of cerebroside sulfate containing palmitic or α-hydroxy palmitic acid. *Chem. Phys. Lipids.* 34:41–53.

Koshy, K. M., and J. M. Boggs. 1996. Investigation of the calcium-mediated interaction between the carbohydrate headgroups of galactosylceramide and galactosylceramide I^3 sulfate by electrospray ionization mass spectrometry. *J. Biol. Chem.* 271:3496–3499.

Koshy, K. M., J. Wang, and J. M. Boggs. 1999. Divalent cation-mediated interaction between cerebroside sulfate and cerebrosides: an investiga-

tion of the effect of structural variations of lipids by electrospray ionization mass spectrometry. *Biophys. J.* 77:306–318.

Kulkarni, V. S., W. H. Anderson, and R. E. Brown. 1995. Bilayer nanotubes and helical ribbons formed by hydrated galactosylceramides: acyl chain and headgroup effects. *Biophys. J.* 89:1976–1986.

Kulkarni, V. S., J. M. Boggs, and R. E. Brown. 1999. Modulation of nanotube formation by structural modifications of sphingolipids. *Biophys. J.* 77:319–330.

Lee, D. C., I. R. Miller, and D. Chapman. 1986. An infrared spectroscopic study of metastable and stable forms of hydrated cerebroside bilayers. *Biochim. Biophys. Acta.* 856:266–270.

Melchior, V., C. J. Hollingshead, and D. L. D. Caspar. 1979. Divalent cations cooperatively stabilize close membrane contacts in myelin. *Biochim. Biophys. Acta.* 554:204–226.

Menikh, A., and M. Fragata. 1993. Fourier transform infrared spectroscopic study of ion binding and intramolecular interactions in the polar head of digalactosyldiacylglycerol. *Eur. Biophys. J.* 22:249–258.

Menikh, A., P-G. Nyholm, and J. M. Boggs. 1997. Characterization of the interaction of Ca^{2+} with hydroxy and non-hydroxy fatty acid species of cerebroside sulfate by Fourier transform infrared spectroscopy and molecular modeling. *Biochemistry.* 36:3438–3447.

Misevic, G. N., and M. M. Burger. 1993. Carbohydrate-carbohydrate interactions of a novel acidic glycan can mediate sponge cell adhesion. *J. Biol. Chem.* 268:4922–4929.

Norton, W. T. 1977. Isolation and characterization of myelin. *In* Myelin. P. Morell, editor. Plenum Press, New York. 161–199.

Pascher, I., and S. Sundell. 1977. Molecular arrangements in sphingolipids: the crystal structure of cerebroside. *Chem. Phys. Lipids.* 20:175–191.

Savitzky, A., and M. J. E. Golay. 1964. Smoothing and differentiation of data by simplified least squares procedures. *Anal. Chem.* 36:1627–1639.

Spillman, D. 1994. Carbohydrates in cellular recognition: from leucine zipper to sugar zipper? *Glycoconj. J.* 11:169–171.

Stewart, R. J., and J. M. Boggs. 1990. The influence of membrane lipid composition on glycolipid surface expression. *Biochemistry.* 29: 3644–3653.

Stewart, R. J., and J. M. Boggs. 1993. The carbohydrate-carbohydrate interaction between galactosylceramide-containing liposomes and cerebroside sulfate-containing liposomes: dependence on the glycolipid ceramide composition. *Biochemistry.* 32:10666–10674.

Tu, A. T. 1982. Raman Spectroscopy in Biology. Principles and Applications. John Wiley and Sons, Inc., New York.